Iterative Joint MMSE Spatial Filtering/Successive MUI Cancellation for Frequency-domain Filtered SC-FDMA Uplink

Suguru OKUYAMA† Kazuki TAKEDA† and Fumiyuki ADACHI‡
Dept. of Electrical and Communication Engineering, Graduate School of Engineering, Tohoku University
6-6-05 Aza-Aoba, Aramaki, Aoba-ku, Sendai, 980-8579 Japan
E-mail: †{okuyama, kazuki}@mobile.ecei.tohoku.ac.jp, ‡adachi@ecei.tohoku.ac.jp

***Abstract*— Frequency-domain filtered single carrier (SC)-FDMA signal has properties of reduced peak-to-average power ratio (PAPR) and increased frequency diversity gain. However, if the carrier-frequency separation is kept the same as in the case of the transmit filter roll-off factor α=0, the adjacent users' signal spectra overlap and the multi-user interference (MUI) is produced. In our previous work, we proposed an iterative joint single-user minimum mean square error frequency-domain equalization/successive MUI cancellation (called iterative joint MMSE-FDE/SMUIC), which performs iteratively a series of MMSE-FDE, spectrum combining, and SMUIC, for frequency-domain filtered SC-FDMA uplink. However, the residual ISI and MUI limit the BER performance improvement. In this paper, we replace the single-user MMSE-FDE by an MMSE spatial filtering (MMSE-SF) and propose an iterative joint multi-user MMSE-SF/SMUIC (called iterative joint MMSE-SF/SMUIC). The achievable bit error rate (BER) and throughput performances are evaluated by computer simulation.**

Keywords-component; SC-FDMA, MMSE spatial filtering, Iterative MUI cancellation, frequency-domain filter

I. INTRODUCTION

The broadband wireless channel is composed of many propagation paths having different time delays and becomes severely frequency-selective [1],[2]. The use of minimum mean square error frequency-domain equalization (MMSE-FDE) can exploit the channel frequency-selectivity to improve the bit error rate (BER) performance [3-5].

To limit the signal bandwidth, the square-root Nyquist filter can be used as transmit/receive filters [2],[6]. As the filter roll-off factor α increases, the peak-to-average power ratio (PAPR) decreases and furthermore, an increased frequency diversity gain can be obtained by making use of the excess bandwidth introduced by the transmit filtering [7].

However, if the carrier-frequency separation is kept the same as in the case of α=0, the adjacent users' signal spectra overlap and the multi-user interference (MUI) is produced, thereby significantly degrading the BER and throughput performances. In [12], we proposed an iterative joint single-user minimum mean square error frequency-domain equalization/successive MUI cancellation (iterative joint MMSE-FDE/SMUIC), which performs iteratively a series of MMSE-FDE, spectrum combining [7], and SMUIC, for frequency-domain filtered SC-FDMA uplink. However, the residual ISI and MUI limit the BER performance improvement.

In this paper, we replace the single-user MMSE-FDE by an MMSE spatial filtering (MMSE-SF) [13] and propose an iterative joint multi-user MMSE-SF/SMUIC (iterative joint MMSE-SF/SMUIC). First, two overlapped signals are separated using MMSE-SF [13] and then, spectrum combining is done to restore the desired user's signal spectrum. Finally, the residual MUI and ISI cancellation is carried out. The above series of operation is repeated sufficient times.

The remainder of this paper is organized as follows. The frequency-domain filtered SC-FDMA uplink signal transmission is presented in Sec. II. In Sec. III, we describe the proposed iterative joint MMSE-SF/SMUIC. In Sec. IV, we discuss the simulation results for PAPR, BER, and throughput performances. Sec. V concludes this paper.

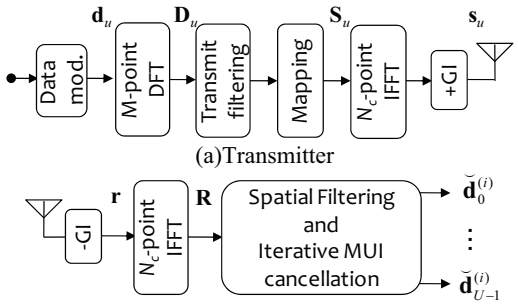

Fig. 1. Transmission system model.

II. FREQUENCY-DOMAIN FILTERED SC-FDMA UPLINK SIGNAL TRANSMISSION

The transmitter/receiver structure of frequency-domain filtered SC-FDMA uplink is illustrated in Fig. 1. Throughout the paper, fast Fourier transform (FFT) sample-spaced discrete-time signal representation is used. A block transmission of M symbols is considered. At the uth(u=0,…,U–1) user transmitter, the data symbol block $\mathbf{d}_u=[d_u(0),\ldots,d_u(M-1)]^T$ is first transformed by M-point discrete Fourier transform (DFT) into the frequency-domain signal $\mathbf{D}_u=[D_u(0),\ldots,D_u(M-1)]^T$. To limit the signal bandwidth, the square root-raised cosine Nyquist filter with the roll-off factor α is applied. The transmit filter transfer function is denoted by $\{H_T(k);k=-M,\ldots,M-1\}$. Here, frequency index range $[-M,M]$ is maximum range of transmit filter (i.e., α=1). The frequency-domain signal after transmit filtering is mapped over N_c subcarriers, where $N_c>>M$ to obtain the frequency-domain signal $\mathbf{S}_u=[S_u(0),\ldots,S_u(N_c-1)]^T$. In this paper, we consider the localized mapping illustrated in Fig. 2. The carrier-frequency separation is kept the same as in the case of α=0 to accommodate the same number of users. The frequency-domain signal after spectrum mapping is transformed back to the time-domain signal by applying N_c-point inverse FFT (IFFT). Last N_g samples of each block are copied as a cyclic prefix and inserted into the guard interval (GI) placed at the beginning of each block.

The GI-inserted signal block is transmitted over a frequency-selective fading channel. At the receiver, the received signal block $\mathbf{r}=[r(0),\ldots,r(N_c-1)]^T$ after the GI removal, is transformed by applying N_c-point FFT into the frequency-domain signal $\mathbf{R}=[R(0),\ldots,R(N_c-1)]^T$. The spatial filtering is carried out on $\mathbf{R}$.

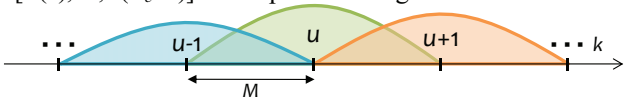

Fig. 2. Spectrum mapping

A. Transmit Signal

The data symbol block $\mathbf{d}_u=[d_u(0),\ldots,d_u(M-1)]^T$ is first transformed by M-point DFT into the frequency-domain signal $\mathbf{D}_u=[D_u(0),\ldots,D_u(M-1)]^T$, to which the frequency-domain transmit filtering and spectrum mapping are applied. The frequency-domain filtered signal $\mathbf{S}_u=[S_u(0),\ldots,S_u(N_c-1)]^T$ is expressed as

978-1-4244-7006-8/10/$26.00 ©2010 IEEE

$$\mathbf{S}_u = \mathbf{P}_u \mathbf{H}_T \mathbf{D}_u = \mathbf{P}_u \mathbf{H}_T \mathbf{F}_M \mathbf{d}_u , \quad (1)$$

where $\mathbf{F}_K$ is an $K \times K$ DFT matrix, given as

$$\mathbf{F}_K = \frac{1}{\sqrt{K}} \begin{bmatrix} 1 & 1 & \cdots & 1 \\ 1 & e^{\frac{-j2\pi \cdot 1 \cdot 1}{K}} & \cdots & e^{\frac{-j2\pi \cdot 1 \cdot (K-1)}{K}} \\ \vdots & \vdots & \ddots & \vdots \\ 1 & e^{\frac{-j2\pi (K-1) \cdot 1}{K}} & \cdots & e^{\frac{-j2\pi (K-1)(K-1)}{K}} \end{bmatrix}, \quad (2)$$

and $\mathbf{H}_T$ is an $2M \times M$ transmit filter matrix, given as

$$\mathbf{H}_T = \begin{bmatrix} H_T(-M) & & & \mathbf{0} \\ & H_T(-M+1) & & \\ & & \ddots & \\ & \mathbf{0} & & H_T(-1) \\ H_T(0) & & & \mathbf{0} \\ & H_T(1) & & \\ & & \ddots & \\ & \mathbf{0} & & H_T(M-1) \end{bmatrix}. \quad (3)$$

In this paper, square root-raised cosine Nyquist filter with roll-off factor α is assumed as the transmit filter, whose transfer function $H_T(k)$ is given by

$$H_T(k) = \begin{cases} 1, & 0 \le |k| < \frac{1-\alpha}{2} M \\ \cos\left[\frac{\pi}{2\alpha}\left(\frac{|k|}{M} - \frac{1-\alpha}{2}\right)\right], & \frac{1-\alpha}{2} M \le |k| < \frac{1+\alpha}{2} M \\ 0, & otherwise \end{cases} . \quad (4)$$

$\mathbf{P}_u$ is an $N_c \times 2M$ mapping matrix, given as

$$\mathbf{P}_u = \begin{bmatrix} \mathbf{0} \\ 1 \\ & \ddots \\ & & 1 \\ \mathbf{0} \end{bmatrix} \Bigg\} 2M . \quad (5)$$

An N_c-point IFFT is applied to $\mathbf{S}_u=[S_u(0),\ldots,S_u(N_c-1)]^T$ to obtain the transmit time-domain signal $\mathbf{s}_u=[s_u(0),\ldots,s_u(N_c-1)]^T$, which is given by

$$\mathbf{s}_u = \sqrt{\frac{2E_{s,u}}{T_s}} \mathbf{F}_{N_c}^H \mathbf{S}_u , \quad (6)$$

where $E_{s,u}$, T_s, and $[.]^H$ denote the symbol energy, symbol duration, and the Hermitian transpose operation, respectively.

B. Received Signal

The propagation channel is assumed to be an L-path block fading channel, each path being subjected to independent fading. Letting $h_{u,l}$ and $\tau_{u,l}$ be respectively the complex-valued path gain and delay time of the lth path (l=0,…,L–1), the channel impulse response is expressed as

$$h_u(\tau) = \sum_{l=0}^{L-1} h_{u,l} \delta(\tau - \tau_{u,l}) , \quad (7)$$

where $\delta(\tau)$ is the delta function. The received signal $\mathbf{r}=[r(0),\ldots,r(N_c-1)]^T$ can be expressed as

$$\mathbf{r} = \sum_{u=0}^{U-1} \mathbf{h}_u \mathbf{s}_u + \mathbf{n} , \quad (8)$$

where $\mathbf{n}=[n(0),\ldots,n(N_c-1)]^T$ is the noise vector with each element is an independent zero-mean complex Gaussian noise with variance $2N_0/T_s$ (N_0 is the single-sided power spectrum density of the additive white Gaussian noise (AWGN)) and $\mathbf{h}_u$ is an $N_c \times N_c$ channel impulse response matrix, given as

$$\mathbf{h}_u = \begin{bmatrix} h_{u,0} & & & h_{u,L-1} & & \\ \vdots & h_{u,0} & & & \ddots & \\ & \vdots & \ddots & \mathbf{0} & & h_{u,L-1} \\ h_{u,L-1} & & & h_{u,0} & & \\ & h_{u,L-1} & & \vdots & \ddots & \\ \mathbf{0} & & \ddots & & & h_{u,0} \end{bmatrix}. \quad (9)$$

N_c-point FFT is applied to $\mathbf{r}=[r(0),\ldots,r(N_c-1)]^T$ to transform it into the frequency-domain signal $\mathbf{R}=[R(0),\ldots,R(N_c-1)]^T$. $\mathbf{R}$ is given by

$$\mathbf{R} = \mathbf{F}_{N_c} \mathbf{r} = \mathbf{F}_{N_c} \sum_{u=0}^{U-1} \mathbf{h}_u \mathbf{s}_u + \mathbf{F}_{N_c} \mathbf{n} . \quad (10)$$

Since the channel impulse matrix $\mathbf{h}_u$ is a circulant matrix, we have

$$\mathbf{F}_{N_c} \mathbf{h}_u \mathbf{F}_{N_c}^H = diag[H_u(0),\ldots,H_u(N_c-1)] \equiv \mathbf{H}_u . \quad (11)$$

Using Eq. (11), Eq. (10) can be rewritten as

$$\mathbf{R} = \overline{\mathbf{H}}\mathbf{D} + \mathbf{N} = \left[\overline{\mathbf{H}}_0 \overline{\mathbf{H}}_1 \ldots \overline{\mathbf{H}}_{U-1}\right]\left[\mathbf{D}_0 \mathbf{D}_1 \ldots \mathbf{D}_{U-1}\right]^T + \mathbf{N} , \quad (12)$$

where $\overline{\mathbf{H}}_u = \mathbf{H}_u \mathbf{P}_u \mathbf{H}_T$ is an $N_c \times M$ equivalent channel matrix and $\mathbf{N}=[N(0),\ldots,N(N_c-1)]^T$ is the noise vector.

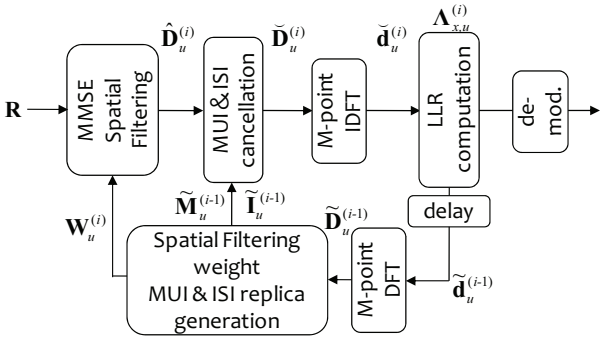

Fig. 3. MMSE spatial filtering using iterative MUI cancellation.

III. ITERATIVE JOINT MMSE SPATIAL FILTERING/ SUCCESSIVE MUI CANCELLARTION

Iterative joint MMSE-SF/SMUIC separates overlapped adjacent users' spectra using MMSE spatial filtering and restores the desired user's signal spectrum by using the spectrum combining [7]. After MMSE spatial filtering, the cancellation of MUI and ISI is performed. The uth user frequency-domain signal $\hat{\mathbf{D}}_u^{(i)} = [\hat{D}_u^{(i)}(0),\ldots,\hat{D}_u^{(i)}(M-1)]^T$ after MMSE spatial filtering at the ith stage is given as

$$\begin{aligned} \hat{\mathbf{D}}_u^{(i)} &= \mathbf{W}_u^{(i)} \mathbf{R} \\ &= \mathbf{W}_u^{(i)} (\overline{\mathbf{H}}_0 \mathbf{D}_0 + \overline{\mathbf{H}}_1 \mathbf{D}_1 + \cdots \overline{\mathbf{H}}_{U-1} \mathbf{D}_{U-1}) + \mathbf{W}_u^{(i)} \mathbf{N} \\ &= \mathbf{W}_u^{(i)} \overline{\mathbf{H}}_u \mathbf{D}_u + \mathbf{W}_u^{(i)} (\overline{\mathbf{H}}_{u-1} \mathbf{D}_{u-1} + \overline{\mathbf{H}}_{u+1} \mathbf{D}_{u+1}) + \mathbf{W}_u^{(i)} \mathbf{N} \end{aligned} , \quad (13)$$

where $\mathbf{W}_u^{(i)}$ is the MMSE spatial filtering weight matrix of size $M \times N_c$ which minimizes the trace $tr[E(\mathbf{e}\mathbf{e}^H)]$ of the covariance matrix of the error vector between $\mathbf{D}_u$ (the transmitted data block) and $\breve{\mathbf{D}}_u^{(i)}$ (the soft decision symbol block after interference cancellation).

Frequency-domain MUI and residual ISI cancellation is carried out simultaneously as

$$\breve{\mathbf{D}}_u^{(i)} = \hat{\mathbf{D}}_u^{(i)} - \widetilde{\mathbf{M}}_u^{(i)} - \widetilde{\mathbf{I}}_u^{(i)} . \quad (14)$$

where $\widetilde{\mathbf{M}}_u^{(i)}$ and $\widetilde{\mathbf{I}}_u^{(i)}$ are respectively the MUI replica and residual ISI replica which will be shown in Sect. III. A.

Finally, the soft decision symbol

$\breve{\mathbf{d}}_u^{(i)} = [\breve{d}_u^{(i)}(0),\ldots,\breve{d}_u^{(i)}(M-1)]^T$ is obtained by applying M-point IDFT to $\breve{\mathbf{D}}_u^{(i)} = [\breve{D}_u^{(i)}(0),\ldots,\breve{D}_u^{(i)}(M-1)]^T$ as

$$\breve{\mathbf{d}}_u^{(i)} = \mathbf{F}_M^H \breve{\mathbf{D}}_u^{(i)}. \quad (15)$$

A. MUI Replica Generation

How to generate MUI replica and residual ISI replica of the uth users at the ith stage is presented below. The receiver structure of MUI cancellation is illustrated in Fig.3. The uth users' received signal power P_u is given by

$$P_u = \frac{1}{M} tr[\overline{\mathbf{H}}_u \overline{\mathbf{H}}_u^H]. \quad (16)$$

$\{P_u; u=0,\ldots,U-1\}$ are compared and signal detection is carried out in the descending order of the received signal power. In this paper, we assume $P_0 \geq P_1 \geq \ldots \geq P_u \geq \ldots \geq P_{U-1}$ without loss of generality. The LLR (log-likelihood ratio) of the xth (x=0,...,N–1) bit in the nth (n=0,…,M–1) symbols in a block (N is the number of bits per symbol) is computed using the decision variable $\{\breve{d}_u^{(i-1)}(n)\}$ [8] as

$$\Lambda_{x,u}^{(i-1)}(n) = \ln\left(\frac{p_u^{(i-1)}(b_{n,x}=1)}{p_u^{(i-1)}(b_{n,x}=0)}\right) \approx \frac{\left|\breve{d}_u^{(i-1)}(n) - \sqrt{\frac{2E_{s,u}}{T_s}} A_u^{(i-1)} d_{b_{n,x}=0}^{\min}\right|^2}{2(\hat{\sigma}_u^{(i-1)})^2} - \frac{\left|\breve{d}_u^{(i-1)}(n) - \sqrt{\frac{2E_{s,u}}{T_s}} A_u^{(i-1)} d_{b_{n,x}=1}^{\min}\right|^2}{2(\hat{\sigma}_u^{(i-1)})^2}, \quad (17)$$

where $p_u^{(i-1)}(b_{n,x}=0)$ and $p_u^{(i-1)}(b_{n,x}=1)$ are the *a posteriori* probabilities of the transmitted bit $b_{n,x}$ being $b_{n,x}$=0 and $b_{n,x}$=1, respectively, at the (i–1)th iteration stage, $d_{b_{n,x}=0}^{\min}$ (or $d_{b_{n,x}=1}^{\min}$) is the symbol whose xth bit is 0 (or 1) and which has the shortest Euclidean distance from $\hat{d}_u^{(i-1)}(n)$, and $2(\hat{\sigma}_u^{(i-1)})^2$ is the variance of MUI, residual ISI plus noise. $2(\hat{\sigma}_u^{(i-1)})^2$ is given by

$$\begin{aligned} 2(\hat{\sigma}_u^{(i)})^2 &= 2(\hat{\sigma}_{u,MUI}^{(i)})^2 + 2(\hat{\sigma}_{u,ISI}^{(i)})^2 + 2(\hat{\sigma}_{u,noise}^{(i)})^2 \\ &= 2\frac{E_{s,u-1}}{T_s}\frac{\rho_{u-1}^{(i)}}{M} tr[(\mathbf{W}_u^{(i)}\overline{\mathbf{H}}_{u-1})(\mathbf{W}_u^{(i)}\overline{\mathbf{H}}_{u-1})^H] \\ &+ 2\frac{E_{s,u+1}}{T_s}\frac{\rho_{u+1}^{(i-1)}}{M} tr[(\mathbf{W}_u^{(i)}\overline{\mathbf{H}}_{u+1})(\mathbf{W}_u^{(i)}\overline{\mathbf{H}}_{u+1})^H] \\ &+ 2\frac{E_{s,u}}{T_s}\frac{\rho_u^{(i-1)}}{M}\left(tr[(\mathbf{W}_u^{(i)}\overline{\mathbf{H}}_u)(\mathbf{W}_u^{(i)}\overline{\mathbf{H}}_u)^H] - |A_u^{(i)}|^2 tr[\mathbf{I}]\right) \\ &+ 2\frac{N_0}{T_s}\frac{1}{M} tr[\mathbf{W}_u^{(i)}\mathbf{W}_u^{(i)H}] \end{aligned}, \quad (18)$$

where

$$A_u^{(i)} = \frac{1}{M} tr[\mathbf{W}_u^{(i)}\overline{\mathbf{H}}_u] \quad (19)$$

and $\rho_u^{(i)}$ is given as [8]

$$\begin{aligned} \rho_u^{(i)} &= E[|D_u(k) - \tilde{D}_u^{(i)}(k)|^2] \\ &\approx \frac{1}{M}\sum_{n=0}^{M-1}\left(E[|d_u(n)|^2] - |\tilde{d}_u^{(i)}(n)|^2\right). \end{aligned} \quad (20)$$

In the above, $E[|d_u(n)|^2]$ is the expectation of the transmitted symbol obtained using the *a posteriori* probabilities, $p_u^{(i-1)}(b_{n,x}=0)$ and $p_u^{(i-1)}(b_{n,x}=1)$, for the given received signal block $\mathbf{r}=[r(0),\ldots,r(N_c-1)]^T$ and is given by [8],

$$E[|d_u(n)|^2] = \begin{cases} 1 & \text{for QPSK} \\ \frac{4}{10}\tanh\left(\frac{\Lambda_{1,u}^{(i-1)}(n)}{2}\right) + \frac{4}{10}\tanh\left(\frac{\Lambda_{3,u}^{(i-1)}(n)}{2}\right) + 1 & \text{for 16QAM} \end{cases}. \quad (21)$$

The soft symbol replica $\{\tilde{d}_u^{(i)}(n)\}$ is given as [8]

$$\begin{cases} \tilde{d}_u^{(i-1)}(n) = \frac{1}{\sqrt{2}}\tanh\left(\frac{\Lambda_{0,u}^{(i-1)}(n)}{2}\right) + j\frac{1}{\sqrt{2}}\tanh\left(\frac{\Lambda_{1,u}^{(i-1)}(n)}{2}\right) & \text{for QPSK} \\ \tilde{d}_u^{(i-1)}(n) = \frac{1}{\sqrt{10}}\tanh\left(\frac{\Lambda_{0,u}^{(i-1)}(n)}{2}\right)\left\{2 + \tanh\left(\frac{\Lambda_{1,u}^{(i-1)}(n)}{2}\right)\right\} & \\ \quad + j\frac{1}{\sqrt{10}}\tanh\left(\frac{\Lambda_{2,u}^{(i-1)}(n)}{2}\right)\left\{2 + \tanh\left(\frac{\Lambda_{3,u}^{(i-1)}(n)}{2}\right)\right\} & \text{for 16QAM} \end{cases}. \quad (22)$$

The soft decision symbol block replica $\tilde{\mathbf{d}}_u^{(i-1)} = [\tilde{d}_u^{(i-1)}(0),\ldots,\tilde{d}_u^{(i-1)}(M-1)]^T$ is transformed into the soft frequency-domain signal $\tilde{\mathbf{D}}_u^{(i-1)} = [\tilde{D}_u^{(i-1)}(0),\ldots,\tilde{D}_u^{(i-1)}(M-1)]^T$ by applying M-point DFT as

$$\tilde{\mathbf{D}}_u^{(i-1)} = \mathbf{F}_M \tilde{\mathbf{d}}_u^{(i-1)}, \quad (23)$$

where $\tilde{d}_u^{(-1)}(n) = 0$. The ($u$–1)th user and the ($u$+1)th user interfere with the desired uth user. The (u–1)th user has been detected. The (u–1)th user's soft decision frequency-domain signal is denoted by $\tilde{\mathbf{D}}_{u-1}^{(i)}$. However, the ($u$+1)th user has not been detected yet in the current ith stage and therefore, the frequency-domain signal regenerated at the previous (i–1)th stage is used for generating the (u+1)th user's MUI replica $\tilde{\mathbf{D}}_{u+1}^{(i-1)}$. MUI cancellation is carried out according to Eq. (14). The frequency-domain MUI replica $\tilde{\mathbf{M}}_u^{(i)} = [\tilde{M}_u^{(i)}(0),\ldots,\tilde{M}_u^{(i)}(M-1)]^T$ and residual ISI replica $\tilde{\mathbf{I}}_u^{(i)} = [\tilde{I}_u^{(i)}(0),\ldots,\tilde{I}_u^{(i)}(M-1)]^T$ are generated as

$$\begin{cases} \tilde{\mathbf{M}}_u^{(i)} = \sqrt{\frac{2E_{s,u-1}}{T_s}}\mathbf{W}_u^{(i)}\overline{\mathbf{H}}_{u-1}\tilde{\mathbf{D}}_{u-1}^{(i)} + \sqrt{\frac{2E_{s,u+1}}{T_s}}\mathbf{W}_u^{(i)}\overline{\mathbf{H}}_{u+1}\tilde{\mathbf{D}}_{u+1}^{(i-1)} \\ \tilde{\mathbf{I}}_u^{(i)} = \sqrt{\frac{2E_{s,u}}{T_s}}\left(\mathbf{W}_u^{(i)}\overline{\mathbf{H}}_u - A_u^{(i)}\mathbf{I}\right)\tilde{\mathbf{D}}_u^{(i-1)} \end{cases}. \quad (24)$$

B. MMSE Spatial Filtering Weight Matrix

MMSE spatial filtering weight matrix is derived which minimizes the trace $tr[\mathrm{E}(\mathbf{e}\mathbf{e}^H)]$ of the covariance matrix of the error vector between the frequency-domain signal after interference cancellation $\tilde{\mathbf{D}}_u^{(i)} = [\tilde{D}_u^{(i)}(0),\ldots,\tilde{D}_u^{(i)}(M-1)]^T$ and the transmit data symbol block $\mathbf{D}_u=[D_u(0),\ldots,D_u(M-1)]^T$. The MMSE spatial filtering weight of uth user at the ith stage is given by [14]

$$\mathbf{W}_u^{(i)} = E_{s,u}\rho_u^{(i-1)}\overline{\mathbf{H}}_u^H\left[E_{s,u-1}\rho_{u-1}^{(i)}\overline{\mathbf{H}}_{u-1}\overline{\mathbf{H}}_{u-1}^H + \sum_{u'=u}^{u+1}E_{s,u'}\rho_{u'}^{(i-1)}\overline{\mathbf{H}}_{u'}\overline{\mathbf{H}}_{u'}^H + N_0\mathbf{I}\right]^{-1}. \quad (25)$$

IV. Computer Simulation

The simulation condition is summarized in Table 1. A block transmission of M=64 and QPSK or 16QAM data modulation is considered. We assume an L=16-path frequency-selective block Rayleigh fading channel having uniform power delay profile (i.e., $E[|h_{u,l}|^2]=1/L$ for all l). It is assumed that the sum of maximum transmit timing offset among users and channel maximum delay time is less than the GI length. Ideal channel estimation and ideal slow transmit power control ($E_{s,u}=E_s$ for all user) are also assumed.

Table. 1 Simulation condition

Transmitter	Data modulation	QPSK, 16QAM
	Number of symbols per block	M=64
	FFT/IFFT block size	N_c=256
	GI length	N_g=32
Transmit/receive filters	Transfer function	Square root-raised cosine
	Roll off factor	α=0~1
Channel	Fading type	Frequency-selective block Rayleigh
	Power delay profile	L=16-path uniform power delay profile
Receiver	Signal detection	MMSE spatial filtering
	Channel estimation	Ideal

A. PAPR

PAPR is defined as [9]

$$\mathrm{PAPR}=\frac{\max\{|s_u(t)|^2\}_{t=0\sim N_c-1}}{E[|s_u(t)|^2]}. \quad (26)$$

The PAPR level at the complementary cumulative distribution function (CCDF)=10^{-3} is shown in Table 2 for various values of the roll-off factor α [12]. As α increases, the $\mathrm{PAPR}_{0.1\%}$ level decreases, but it becomes almost the same beyond α=0.5.

Table. 2 PAPR level at CCDF=10^{-3}

α		0	0.25	0.5	0.75	1
$\mathrm{PAPR}_{0.1\%}$ (dB)	QPSK	7.54	4.68	3.47	3.44	3.62
	16QAM	8.44	6.74	6.03	6.34	6.48

B. BER performance

The impact of the number i of iterations on BER with α=1 is plotted for iterative joint MMSE-FDE/SMUIC [12] and iterative joint MMSE-SF/SMUIC in Fig. 4 when the average received bit energy-to-noise power spectrum density ratio E_b/N_0=12(18)dB for QPSK (16QAM), where E_b/N_0 given by $(1/N)(1+N_g/N_c)(E_s/N_0)$ with N being the number of bits per symbol. For comparison, the BER is also plotted for the single-user case (note that iterative ISIC [8] is used). As the number of iterations, i, increases, the BER reduces for both iterative joint MMSE-FDE/SMUIC and iterative joint MMSE-SF/SMUIC. However, the proposed iterative joint MMSE-SF/SMUIC can achieve better BER performance than iterative joint MMSE-FDE/SMUIC and achieve the BER performance close to the single-user case. In the case of 16QAM data modulation, iterative joint MMSE-FDE/SMUIC produces BER floor even if a large number of iterations is used. This is because the Euclidean distance between the adjacent 16QAM symbols in the signal constellation is small and hence the error propagation occurs even if a small amount of residual MUI is present. However, by replacing the single-user MMSE-FDE by multi-user MMSE spatial filtering, iterative joint MMSE-SF/SMUIC can sufficiently suppress the MUI when i=3 and can achieve BER performance close to the single-user case.

The BER performance when α=1 is plotted for iterative joint MMSE-FDE/SMUIC [12] and iterative joint MMSE-SF/SMUIC in Fig. 5 as a function of the average received E_b/N_0 with three iterations (i=3). For comparison, the BER performance for the single-user case (note that iterative ISIC [8] is used) and the matched filter bound are also plotted. First, let discuss about the BER performance improvement when QPSK data modulation is used. The proposed iterative joint MMSE-SF/SMUIC can achieve BER performance close to the single-user case and the E_b/N_0 degradation for BER=10^{-4} from the MF bound is as small as 2dB. However, previously proposed iterative joint MMSE-FDE/SMUIC [12] produces BER floors. When 16QAM data modulation is used, the proposed iterative joint MMSE-SF/SMUIC provides a good BER performance while the BER performance of iterative joint MMSE-FDE/SMUIC degrades significantly.

The simulated BERs using iterative joint MMSE-FDE/SMUIC (i=5) and iterative joint MMSE-SF/SMUIC (i=3) are plotted in Fig. 6 as a function of roll-off factor α when E_b/N_0=12 (18) dB for QPSK (16QAM). For comparison, the simulated BER is also plotted for the single-user case (iterative ISIC [8] is used). As α increases, the BER reduces since additional frequency diversity gain can be obtained by exploiting the excess bandwidth introduced by transmit filtering. It can be seen from Fig. 6(a) that when QPSK data modulation is used, both iterative joint MMSE-FDE/SMUIC and iterative joint MMSE-SF/SMUIC can achieve the BER close to the single-user case. It can be seen from Fig. 6(b) that when 16QAM data modulation is used, iterative joint MMSE-SF/SMUIC can achieve close to the single-user case and the BER reduces as α increases; however, the BER using iterative joint MMSE-FDE/SMUIC increases as α increases. The BER performance improvement by using the previously proposed iterative joint MMSE-FDE/SMUIC is limited when 16QAM is used. However, the proposed iterative joint MMSE-SF/SMUIC can sufficiently reduce the MUI through the use of multi-user MMSE spatial filtering instead of the single-user MMSE-FDE and accordingly, can achieve the BER close to the single-user case even if 16QAM is used.

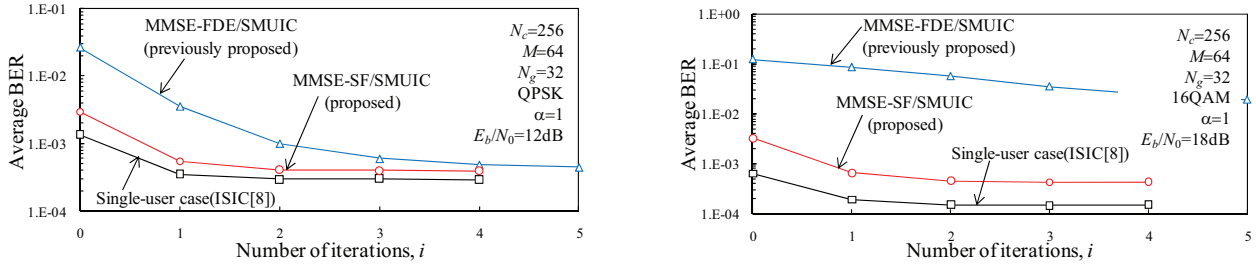

(a) QPSK (b) 16QAM

Fig.4 Impact of the number of iterations, i.

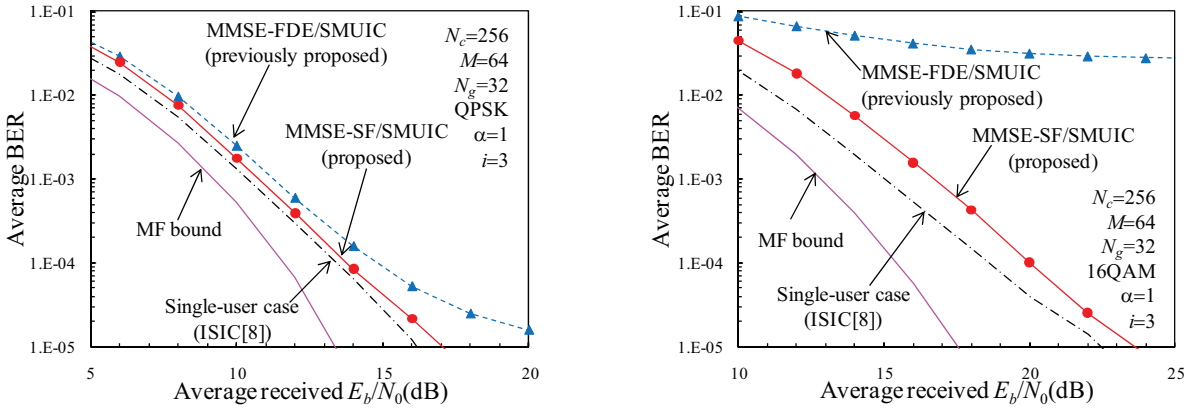

(a) QPSK (b) 16QAM

Fig. 5 BER performance for α=1

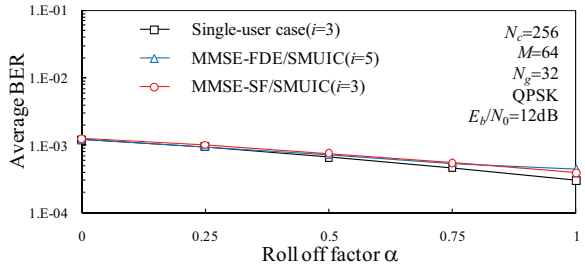

(a) QPSK

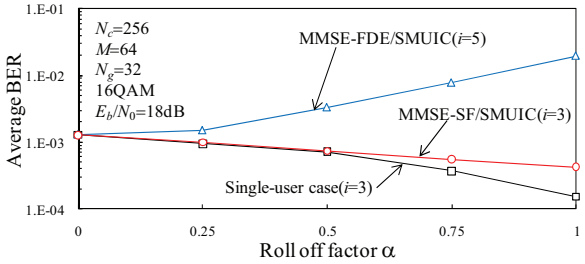

(b) 16QAM

Fig.6 Impact of roll off factor, α.

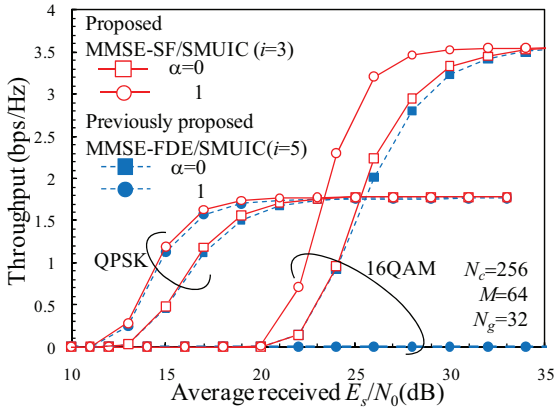

Fig. 7 Throughput vs. average received E_s/N_0

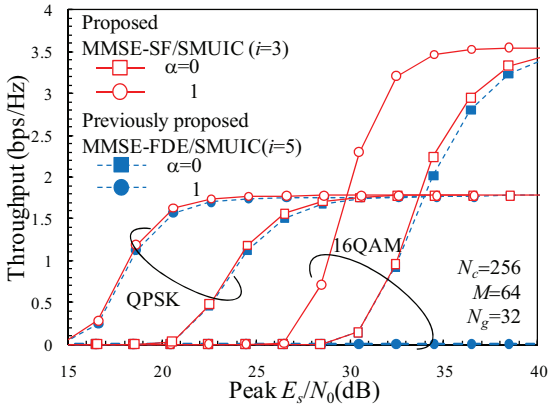

Fig. 8 Throughput vs. peak E_s/N_0

C. *Throughput performance*

Packet error rate (PER) was measured when iterative joint MMSE-SF/SMUIC with i=3 is used. Each packet is assumed to consist of 1024 bits. The throughput η(bps/Hz) is defined [11]

$$\eta = N \times (1 - \mathrm{PER}) \times (1 + N_g / N_c)^{-1}. \quad (27)$$

The throughput performance for α=0,1 is plotted as a function of the average received E_s/N_0 in Fig. 7. For comparison, the throughput performance using previously proposed iterative joint MMSE-FDE/SMUIC [12] with i=5 is also plotted. When QPSK data modulation is used, both iterative joint MMSE-FDE/MUIC and iterative joint MMSE-SF/SMUIC achieve almost the same throughput performance. It can be seen that as α increases, the throughput performance improves. This is because both schemes can obtain the additional frequency diversity gain while sufficiently suppressing both MUI and ISI. It is interesting to note that when 16QAM data modulation is used, iterative joint MMSE-SF/SMUIC can achieve larger performance improvement than iterative joint MMSE-FDE/SMUIC.

The peak E_s/N_0 is an important parameter which determines the peak transmit power required for the mobile terminal transmitter power amplifiers. In this paper, peak E_s/N_0 is defined as peak E_s/N_0=average received E_s/N_0 + $\mathrm{PAPR}_{0.1\%}$ [10]. The throughput performance is plotted as a function of peak E_s/N_0 in Fig. 8. It can be seen from Fig. 8 that the throughput performance improvement is more pronounced due to the reduced PAPR.

V. Conclusion

In this paper, we proposed an iterative joint MMSE-spatial filtering/successive MUI cancellation (called iterative joint MMSE-SF/SMUIC), which performs iteratively a series of multi-user MMSE spatial filtering, spectrum combining, and MUI cancellation, for frequency-domain filtered SC-FDMA uplink. In MMSE-SF, the signal detection is done successively according to the user ranking based on the received signal power measurement. The PAPR, BER and throughput performance using the proposed scheme were evaluated by computer simulation. As the filter roll-off factor α increases, the PAPR decreases. The proposed iterative joint MMSE-SF/SMUIC can achieve better BER performance than previously proposed iterative joint MMSE-FDE/SMUIC. The BER performance close to the single user case can be achieved with the proposed scheme even if 16QAM data modulation is used. As the filter roll-off factor α increases, the throughput performance improves since larger frequency diversity gain is obtained. The throughput improvement is more pronounced when the throughput performance vs. peak E_s/N_0 is considered.

References

[1] W. C., Jakes Ir., Ed,. *Microwave mobile communications*, Wiley, New York, 1974.
[2] J. G. Proakis, Digital communications, 4th ed., McGraw-Hill, 2001.
[3] D. Falconer, S. L. Ariyavisitakul, A. Benyamin-Seeyarand B. Edison, "Frequency domain equalization for single-carrier broadband wireless systems," IEEE Commun. Mag., Vol.40, No. 4, pp.58-66. Apr. 2002.
[4] F. Adachi, D. Garg, S. Takaoka, and K. Takeda, "Broadband CDMA techniques," IEEE Wireless Commun., Mag., Vol. 12, No. 2, pp. 8-18, Apr. 2005.
[5] F. Adachi and K. Takeda, "Bit error rate analysis of DS-CDMA with joint frequency-domain equalization and antenna diversity reception," IEICE Trans. Commun., Vol. E87-B, No. 10, pp. 2991-3002, Oct. 2004.
[6] Y. Akaiwa, *Introduction to digital mobile communication*, Wiley, New York, 1997.
[7] S. Okuyama, K, Takeda and F, Adachi, "MMSE frequency-domain equalization using spectrum combining for Nyquist filtered broadband single-carrier transmission," Proc. IEEE 71st Veh. Technol. Conf. (VTC2010-spring), May 2010.
[8] K. Takeda, K. Ishihara and F. Adachi, "Frequency-Domain ICI Cancellation with MMSE Equalization for DS-CDMA Downlink," IEICE Trans. Commun., Vol.E89-B No.12, pp.3335-3343, Dec. 2006.
[9] H. G. Myung, J. Lim, and D. J. Goodman, "Single Carrier FDMA for Uplink Wireless Transmission", *IEEE Vehicular Technology Magazine*, vol. 3, no. 1, Sep. 2006, pp. 30-38.
[10] H. Gacanin and F. Adachi, "A Comprehensive Performance Comparison of OFDM/TDM Using MMSE-FDE and Conventional OFDM," Proc. IEEE 67th Veh. Technol. Conf. (VTC), pp.11-14, May, 2008.
[11] K. Fukuda, A. Nakajima, and F. Adachi, "LDPC-coded HARQ Throughput Performance of MC-CDMA using ICI Cancellation," Proc. IEEE 66th Veh. Technol. Conf. (VTC), pp.965-969, Sep. 2007.
[12] S. Okuyama, K, Takeda and F, Adachi, "Frequency-domain Iterative MUI Cancellation for Uplink SC-FDMA Using Frequency-domain Filtering," Proc. IEEE 72nd Veh. Technol. Conf. (VTC2010-fall), Sep. 2010.
[13] E. Biglieri, R. Calderbank, A. Constantinides, A.Goldsmith, A. Paulraj, and H. Vincent Poor, *MIMO Wireless Communications*, Cambridge University Press, 2007.
[14] A. Nakajima and F. Adachi, "Iterative Joint PIC and 2D MMSE-FDE for Turbo-coded HARQ with SC-MIMO Multiplexing," Proc. IEEE 63th Veh. Technol. Conf. (VTC), May. 2006.